Vol 466|5 August 2010|doi:10.1038/nature09257

LETTERS

Melting-induced stratification above the Earth's inner core due to convective translation

Thierry Alboussière[1,2], Renaud Deguen[1,3] & Mickaël Melzani[1]

In addition to its global North–South anisotropy[1], there are two other enigmatic seismological observations related to the Earth's inner core: asymmetry between its eastern and western hemispheres[2–6] and the presence of a layer of reduced seismic velocity at the base of the outer core[6–12]. This 250-km-thick layer has been interpreted as a stably stratified region of reduced composition in light elements[13]. Here we show that this layer can be generated by simultaneous crystallization and melting at the surface of the inner core, and that a translational mode of thermal convection in the inner core can produce enough melting and crystallization on each hemisphere respectively for the dense layer to develop. The dynamical model we propose introduces a clear asymmetry between a melting and a crystallizing hemisphere which forms a basis for also explaining the East–West asymmetry. The present translation rate is found to be typically 100 million years for the inner core to be entirely renewed, which is one to two orders of magnitude faster than the growth rate of the inner core's radius. The resulting strong asymmetry of buoyancy flux caused by light elements is anticipated to have an impact on the dynamics of the outer core and on the geodynamo.

The original observation[7] of seismic compressional (P)-wave velocities slower than the adiabatic PREM[14] model in the lower outer core has since been confirmed and incorporated in one-dimensional global models AK135 (ref. 10) and PREM2 (ref. 11). That discrepancy from the adiabatic profile could result from a wrong interpretation caused by the nearby complex inner core, because sensitivity kernels have a width of several hundred kilometres at body-wave frequencies[15], or might also be attributed to floating crystals[12,16]. Gubbins *et al.*[13] show that this last explanation is not possible but that the observed seismic velocities can be explained by a stratification in light elements (and temperature). However, the stratification mechanism by crystallization and melting of crystals at different depths has not been completely elucidated.

We propose that a dense layer can develop when melting and crystallization occur only at the inner-core boundary (ICB). Where crystallization takes place, light elements are released, providing light fluid; where melting takes place, dense fluid is produced. It is possible to quantify these effects in terms of flux of buoyancy. Let us denote $\Delta\rho$ as the fraction of density jump across the ICB that is due to composition partition between solid and liquid phases. For a rate of crystallization V, the buoyancy flux is $\Delta\rho g_c V$, where g_c is the magnitude of gravity[17] on the ICB (subscript c is for 'core'). For melting, the buoyancy flux is $-\Delta\rho g_c V$. The idea is that part of the heavy fluid would remain at the bottom, while the rest would be entrained by the light fluid. Conversely, part of the light fluid would mix with the dense fluid in the dense layer while the rest would cross the dense layer and contribute to convection within the main part of the outer core. This idea has been validated experimentally as follows.

The experiments consist of simultaneously injecting constant fluxes of light and dense fluids at the bottom of a fluid cavity. The cavity is a box of perspex 20 cm high and with a 15 cm × 15 cm horizontal cross-section. It is initially filled with salted water (initial concentration χ_0, in wt% NaCl). At the bottom of the cavity, there is a porous layer (sponge) below which the cross-section is divided into two disconnected parts: on one side light fluid is injected ($\chi_l < \chi_0$) and on the other side heavy fluid is injected ($\chi_h > \chi_0$), where χ_l and χ_h are the salt concentrations of the light and heavy fluids in wt% NaCl. Both density differences $\chi_0 - \chi_l$ and $\chi_h - \chi_0$ and both flow rates are controlled and set to be constant during the experiment. The injections of fluids start simultaneously through pipes from reservoirs with the desired concentration. The excess fluid is removed through an overflow at the top of the cavity.

The geophysically relevant case is when the positive buoyancy flux exceeds the negative one, because on average the inner core is growing. When the negative buoyancy flux induced by the heavy fluid is less than 80% of the amplitude of the light fluid, no dense layer is observed: the entrainment caused by the rise of light plumes is sufficient to mix the heavy fluid as it is released by the bottom boundary. However, when the heavy buoyancy flux is more than 80% of the light buoyancy flux, a dense layer grows at the bottom of the cavity. It has been observed experimentally that the condition for the existence of the dense layer is really a condition for the buoyancy fluxes, as described above; it does not specifically depend either on the volume flow rates or on the density differences between the fluids. This justifies our convection experiment as an appropriate model of a melting/crystallization process for the inner core.

On Fig. 1, an experimental run is shown. This experiment corresponds to a case in which the heavy fluid buoyancy flux was 83% that of the light fluid. The initial concentration and concentrations of the dense and light injected fluids were $\chi_0 = 4$ wt%, $\chi_h = 6$ wt% and $\chi_l = 1.65$ wt% NaCl respectively. The volume flow rate of the dense fluid was $Q_h = 3.9 \times 10^{-7}\,m^3\,s^{-1}$ and that of the light fluid was $Q_l = 4.0 \times 10^{-7}\,m^3\,s^{-1}$. The experiment was run twice under the same conditions: in the first instance, the injected dense fluid was coloured with potassium permanganate and photographs of the set-up were taken at different times after the beginning of the injections. A dense coloured layer forms at the bottom and its thickness grows linearly with time. It is also possible to see convection plumes going up on the right-hand side, carrying along some of the heavy coloured fluid in the upper part of the cavity. In the second instance, the synthetic schlieren method has been used[18,19], providing a quantitative two-dimensional field of refraction index with which to visualize the concentration gradients: their horizontal components are shown on the middle row of Fig. 1, showing convection plumes of light fluid on the right-hand side of the cavity, while their vertical components are shown on the bottom row, visualizing the dense layer and its

[1]Laboratoire de Géophysique Interne et Tectonophysique, CNRS, Observatoire de Grenoble, Université Joseph Fourier, Maison des Géosciences, BP 53, 38041 Grenoble Cedex 9, France. [2]Université de Lyon, CNRS UMR5570, site UCB Lyon 1, 2 rue Raphaël Dubois, bâtiment Géode, 69622 Villeurbanne, Université Lyon 1, ENS de Lyon, France. [3]Department of Earth and Planetary Sciences, Johns Hopkins University, Baltimore, Maryland 21218, USA.

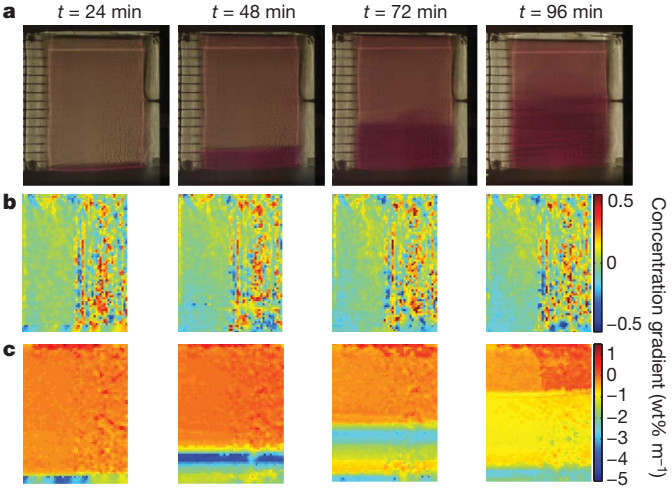

Figure 1 | Visualization of the growth of a dense layer in an experimental run. We used dye injection (**a**) and measurement of horizontal (**b**) and vertical (**c**) density gradients. The experimental cavity is initially filled with a 4 wt% NaCl water solution. From $t = 0$, a constant flux of 1.65 wt% NaCl solution is injected at the bottom on the right-hand side of the cavity while a 6 wt% NaCl solution is injected on the left-hand side. The dense fluid is coloured with potassium permanganate (**a**), visualizing a growing dense layer at the bottom, at four different times after the injection of the dye. The synthetic schlieren method is used in a second identical experiment: the horizontal gradient of refraction index in **b** highlights the convective plumes and the vertical gradient in **c** reveals the dense layer.

growth. The concentration field is computed from its gradient, and averaged along the horizontal direction: the resulting stratification profile is shown in Fig. 2. There is clearly a region of stratified fluid, above which density is nearly uniform. The thickness of this layer grows linearly with time, its volume being 50% to 90% that of the total volume generated by the light and heavy fluxes.

Melting part of the inner core at a significant rate is difficult while it is crystallizing (on average over its surface) as a result of secular cooling. The most plausible mechanism is that a topography is formed dynamically on the ICB so that the temperature of the adjacent fluid of the outer core exceeds the melting temperature. That excess temperature is then responsible for heat transfer from the outer core to the ICB, providing latent heat for fusion: in this way topography can be related to the rate of melting.

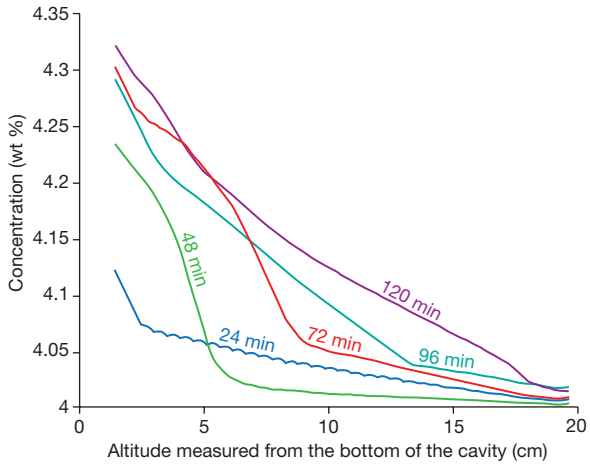

Figure 2 | Evolution of the concentration profile during the growth of a dense layer. The concentration field is extracted from the gradient of refraction index. It is averaged along the horizontal direction and shows the time evolution of the dense layer since injection of the dye.

The dynamical model we put forward to account for significant melting on the ICB results from the combination of three physical elements: the thermal state of a superadiabatic inner core, gravitational equilibrium and finite heat exchange of latent heat with the outer core. In superadiabatic conditions, a uniform velocity in the inner-core V, say from west to east along the x-axis (see Fig. 3), generates a global superadiabatic temperature gradient in the same direction proportional to the residence time in the inner core; such a gradient would hence be inversely proportional to V, and proportional to a positive source term $S \approx 10^{-15}\,\mathrm{K\,s^{-1}}$ defined by secular cooling and thermal conduction along the adiabat (see Methods and ref. 20):

$$\frac{\partial \Theta}{\partial x} = \frac{S}{V} \qquad (1)$$

where Θ is the temperature relative to the adiabat T_{ad} in the inner core anchored to the ICB[17]. It follows from the volume expansion coefficient[21] $\alpha = 1.1 \times 10^{-5}\,\mathrm{K^{-1}}$ and inner-core density (on the ICB[17]) $\rho_s = 1.28 \times 10^{4}\,\mathrm{kg\,m^{-3}}$ (subscript s is for 'solid') that there exists a density gradient $-\alpha\rho_s\partial\Theta/\partial x$. The resulting gravity field and density distribution generate unbalanced forces on the inner core, so that it is displaced a distance δ in the x direction. In the Methods, we derive the gravitational field and potential associated with this mass distribution, from which it is possible to calculate the net gravitational force $\mathbf{F}_G$ exerted on the inner core and the net pressure force $\mathbf{F}_P$ exerted by the outer core on the inner core

$$\mathbf{F}_G + \mathbf{F}_P = \frac{16\,\pi^2}{9} G\,\rho_l c^3 \left[\alpha \frac{\partial \Theta}{\partial x}\rho_s \frac{c^2}{5} - (\rho_s - \rho_l)\delta\right] \mathbf{e}_x \qquad (2)$$

where G is the universal gravitational constant, $c = 1{,}220$ km is the radius of the inner core[17], $\rho_l = 1.22 \times 10^4\ \mathrm{kg\ m^{-3}}$ is the outer core density on the ICB[17] and $\mathbf{e}_x$ is the unit vector in the direction of the

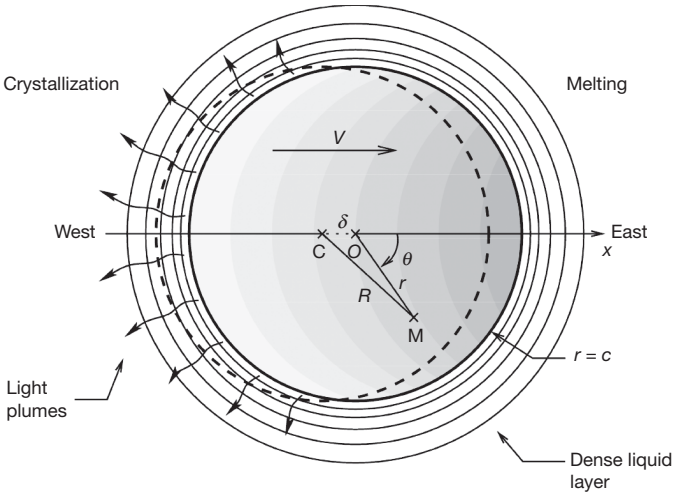

Figure 3 | A schematic representation of the translational convective mode. The centre of the inner core O is shifted by a distance δ away from the centre of the Earth C, which would be its equilibrium position if its density were uniform. That shift causes a thermal departure from the adiabat at the ICB, generating melting on one side and crystallization on the other side. Hence a uniform flow exists in the inner core (arrow labelled V): in the case of a superadiabatic regime, a gradient of temperature develops, as represented by greyscale shading. Its associated changes in density and gravitational potential lead to a new mechanical equilibrium for the inner core, corresponding to a shift in position in the same direction as initially assumed. r is the distance from the centre O of the inner core and θ is the angle between the x axis and the direction of the point where Θ is evaluated. V is the rate of crystallization, and c is the radius of the core. R is the distance between the point at which the gravitational potential U is calculated and the centre of the Earth C. M is a dummy point, used to define r, Θ and R. The dotted circle is the position of the ICB in the absence of density gradient (centred on C). See Methods.

temperature gradient. The equilibrium condition that both forces balance provides the shift δ as a function of the thermal gradient $\partial\Theta/\partial x$

$$\delta = \frac{\alpha \frac{\partial \Theta}{\partial x} \rho_s c^2}{5(\rho_s - \rho_l)} \quad (3)$$

Then, the displacement δ is associated with a non-uniform pressure distribution on the ICB (see Methods), yielding a small temperature departure δT from the adiabat (see Fig. 4)

$$\delta T = \rho_l g_c \, \delta \cos\theta \, (m_P - m_{ad}) \quad (4)$$

where $m_P = 8.5 \times 10^{-9}\,\mathrm{K\,Pa^{-1}}$ is the Clapeyron slope[22], $m_{ad} = (\alpha T_{ad})/(\rho c_p) = 6 \times 10^{-9}\,\mathrm{K\,Pa^{-1}}$ is the adiabatic gradient, $g_c = G\frac{4\pi}{3}\rho_s c$ is the gravity on the ICB and $c_p = 850\,\mathrm{J\,kg^{-1}\,K^{-1}}$ is the specific heat capacity[23]. That departure is accommodated by a thermal boundary layer in the outer core, with a corresponding heat transfer of typical magnitude $u' c_p \delta T$, where $u' = 10^{-4}\,\mathrm{m\,s^{-1}}$ is a typical velocity scale in the outer core. That heat transfer must be balanced by the release or absorption of latent heat

$$L\, V \cos\theta = u' c_p \delta T \quad (5)$$

where $L = 900\,\mathrm{kJ\,kg^{-1}}$ is the latent heat coefficient[24,25]. Finally, combining equations (1), (3), (4) and (5), we can express the translational velocity as

$$V^2 = \frac{4\pi G}{15} \frac{u'\, c_p\, \rho_s^2 \rho_l\, \alpha\, (m_P - m_{ad})\, S}{L\, (\rho_s - \rho_l)} c^3 \quad (6)$$

Depending on the heat flux at the core–mantle boundary, the history of the inner core shows a first phase dominated by growth $\dot{c} \propto c^{-1}$, followed by the development of the translational instability (see Supplementary Information), when its radius was around 400 km, leading to the dominant present translation $V \propto c^{3/2}$ of the order of $5 \times 10^{-10}\,\mathrm{m\,s^{-1}}$, while the growth rate is of the order of $10^{-11}\,\mathrm{m\,s^{-1}}$ (Fig. 5).

The latter scaling law implies that the translational convection is faster along a long axis of the inner-core oblate spheroid (see Supplementary Information), that is, perpendicular to the rotation axis. It follows that the temperature gradient is preferentially aligned with such a long axis, which again reinforces convection in that direction. Moreover, the Earth's aspherical mass distribution—which has essentially a degree 2, order 2 geometry[26]—is responsible for elongating the inner core slightly along an east–west axis and induces a degree 1 translational convection in the inner core through a bifurcation produced by instability (see Supplementary Information). We propose that the translational flow has a west to east orientation, which is responsible for the observed hemispherical asymmetry of the inner core: grain growth during the transit from the western hemisphere to the eastern hemisphere may explain the difference in seismic properties[27]. The temperature difference of a few kelvin between the hemispheres is another source of asymmetry.

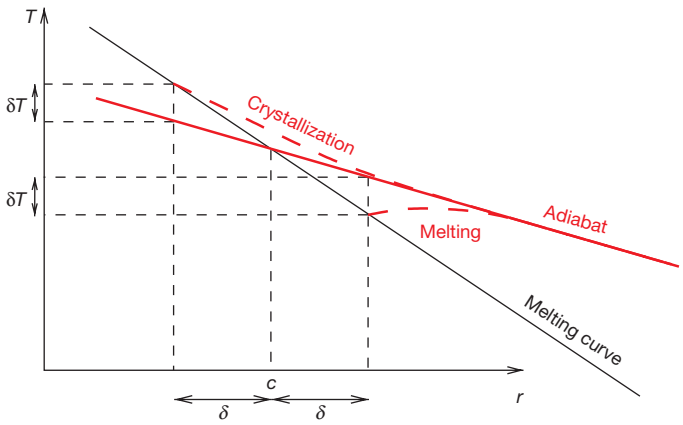

Figure 4 | Thermal departure from the adiabat due to the displacement of the inner core and heat transfer at the ICB. A thermal boundary layer forms in the outer core to adjust to the different radii of the ICB on the melting and crystallization sides.

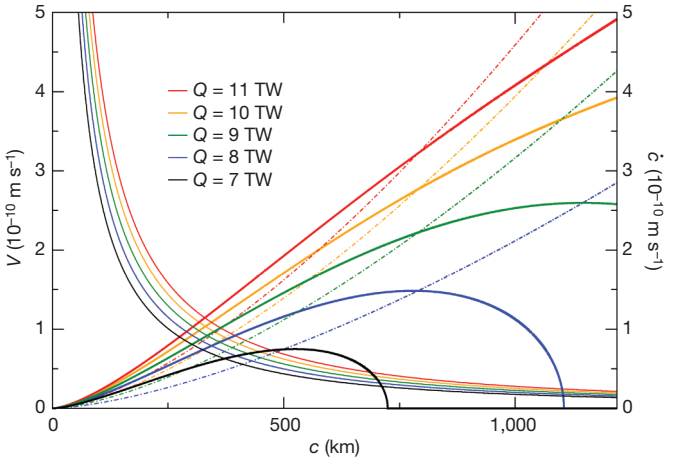

Figure 5 | Growth rate of the radius of the inner core and uniform convective velocity as functions of the inner-core radius. They are plotted for different values of the heat flux Q at the core–mantle boundary. Thin solid lines show the mean solidification (crystallization) rates $\dot{c}$ of the inner core. Dash-dotted lines show the translation velocities V, calculated with the assumption of a constant S. Thick solid lines show the translation velocities V, with $S(t)$ calculated (see Supplementary Information) from the core thermal evolution model of ref. 30.

According to our experiments, a melting rate above 80% of the crystallization rate is necessary for a dense layer to form, which geometrically implies that the translation velocity V is more than 20 times that of the inner-core growth rate. From Fig. 5, we see that this happens only when the core–mantle boundary heat flux exceeds 10 TW, and only since the inner-core radius was 1,100 km, some 200 million years ago. Extrapolating from our experiments, 50% of the volume of melt produced since then would correspond to a layer 250 km thick. The experimental excess concentration is found to be 10% of the concentration difference between light and heavy injected fluids. In the Earth's core, where the concentration of light elements is about 10%, a difference in concentration of around 1% across the dense layer is expected. This is indeed coherent with the observed seismic velocities[13].

Our convection mechanism ignores deformation in the inner core and compositional buoyancy. With a finite effective viscosity, temperature variations along gravity isopotentials induce an internal flow with deformation that affects the translational mode. We have estimated that the internal flow is weak compared to translation for an effective viscosity above 10^{18} Pa s. Enrichment in light elements of the outer core (a few per cent) has been invoked[28,29] to imagine a stabilizing mechanism for convection in the inner core. This is speculative, however, because the fraction of light elements incorporated in the inner core may have decreased more rapidly than the fraction of light elements incorporated into the outer core increased, given that gravity on the ICB is getting larger, reinforcing convection and compaction in the mush.

Invoking an excessively asymmetric buoyancy flux on the ICB calls for further study of the dynamics of the outer core and the geodynamo. The stratified layer is expected to be dynamically isolated and to act as a filter between the inner core and the rest of the outer core, but there might subsist some hemispherical asymmetry in the outer-core dynamics.

METHODS SUMMARY

The mode of convection associated with the translation of the inner core is not standard. Therefore, it is presented in the Methods. Thermal buoyancy is the driving force; however, unlike classical convection, the damping is not due to

viscous and/or thermal diffusion. Damping is set by the capacity of the outer core to extract or supply latent heat on the ICB.

Full Methods and any associated references are available in the online version of the paper at www.nature.com/nature.

Received 7 December 2009; accepted 7 June 2010.

1. Poupinet, G., Pillet, R. & Souriau, A. Possible heterogeneity of the Earth's core deduced from PKIKP travel times. *Nature* **305,** 204–206 (1983).
2. Tanaka, S. & Hamaguchi, H. Degree one heterogeneity and hemispherical variation of anisotropy in the inner core from PKP(BC)-PKP(DF) times. *J. Geophys. Res.* **102,** 2925–2938 (1997).
3. Creager, K. C. Large-scale variations in inner core anisotropy. *J. Geophys. Res.* **104,** 309–314 (1999).
4. Garcia, R. & Souriau, A. Inner core anisotropy and heterogeneity level. *Geophys. Res. Lett.* **27,** 3121–3124 (2000).
5. Niu, F. & Wen, L. Hemispherical variations in seismic velocity at the top of the Earth's inner core. *Nature* **410,** 1081–1084 (2001).
6. Yu, W.-c., Wen, L. & Niu, F. Seismic velocity structure in the earth's outer core. *J. Geophys. Res.* **110,** B02302, doi 10.1029/2003JB002928 (2005).
7. Souriau, A. & Poupinet, G. The velocity profile at the base of the liquid core from PKP(BC+Cdiff) data: an argument in favor of radial inhomogeneity. *Geophys. Res. Lett.* **18,** 2023–2026 (1991).
8. Kennett, B. L. N. & Engdahl, E. R. Traveltimes for global earthquake location and phase identification. *Geophys. J. Int.* **105,** 429–465 (1991).
9. Souriau, A. & Roudil, P. Attenuation in the uppermost inner core from broad-band GEOSCOPE PKP data. *Geophys. J. Int.* **123,** 572–587 (1995).
10. Kennett, B. L. N., Engdahl, E. R. & Buland, R. Constraints on seismic velocities in the earth from traveltimes. *Geophys. J. Int.* **122,** 108–124 (1995).
11. Song, X. & Helmberger, D. V. A. P wave velocity model of Earth's core. *J. Geophys. Res.* **100,** 9817–9830 (1995).
12. Zou, Z., Koper, K. D. & Cormier, V. F. The structure of the base of the outer core inferred from seismic waves diffracted around the inner core. *J. Geophys. Res.* **113,** B05314, doi 10.1029/2007JB005316 (2008).
13. Gubbins, D., Masters, G. & Nimmo, F. A thermochemical boundary layer at the base of Earth's outer core and independent estimate of core heat flux. *Geophys. J. Int.* **174,** 1007–1018 (2008).
14. Dziewonski, A. M. & Anderson, D. L. Preliminary reference Earth model. *Phys. Earth Planet. Inter.* **25,** 297–356 (1981).
15. Calvet, M., Chevrot, S. & Souriau, A. P-wave propagation in transversely isotropic media: II. Application to inner core anisotropy: effect of data averaging, parametrization and a priori information. *Phys. Earth Planet. Inter.* **156,** 21–40 (2006).
16. Loper, D. & Roberts, P. A study of conditions at the inner core boundary of the Earth. *Phys. Earth Planet. Inter.* **24,** 302–307 (1981).
17. Dziewonski, A. M. & Anderson, D. L. Preliminary reference Earth model. *Phys. Earth Planet. Inter.* **25,** 297–356 (1981).
18. Dalziel, S. B., Hughes, G. O. & Sutherland, B. R. Whole-field density measurements by 'synthetic schlieren'. *Exp. Fluids* **28,** 322–335 (2000).
19. Gostiaux, L. & Dauxois, T. Laboratory experiments on the generation of internal tidal beams over steep slopes. *Phys. Fluids* **19,** 028102, doi 10.1063/1.2472511 (2007).
20. Stacey, F. D. & Davis, P. M. *Physics of the Earth* Ch. 19 (Cambridge University Press, 2008).
21. Vočadlo, L. in *Treatise on Geophysics* (ed. Schubert, G.) Vol. 2, 91–120 (2007).
22. Alfè, D., Price, G. D. & Gillan, M. J. Iron under Earth's core conditions: liquid-state thermodynamics and high-pressure melting curve from ab initio calculations. *Phys. Rev. B* **65,** 165118, doi 10.1103/PhysRevB.65.165118 (2002).
23. Poirier, J.-P. Physical properties of the Earth's core. *C. R. Acad. Sci.* **318,** 341–350 (1994).
24. Poirier, J.-P. & Shankland, T. J. Dislocation melting of iron and the temperature of the inner core boundary, revisited. *Geophys. J. Int.* **115,** 147–151 (1993).
25. Anderson, O. L. & Duba, A. Experimental melting curve of iron revisited. *J. Geophys. Res.* **102,** 22659–22670 (1997).
26. Masters, G., Jordan, T. H., Silver, P. G., &. Gilbert, F. Aspherical Earth structure from fundamental spheroidal-mode data. *Nature* 298 609–613 (1982).
27. Calvet, M. & Margerin, L. Constraints on grain size and stable iron phases in the uppermost inner core from multiple scattering modeling of seismic velocity and attenuation. *Earth Planet. Sci. Lett.* **267,** 200–212 (2008).
28. Buffett, B. A. Onset and orientation of convection in the inner core. *Geophys. J. Int.* **179,** 711–719 (2009).
29. Deguen, R. & Cardin, P. Tectonic history of the Earth's inner core preserved in its seismic structure. *Nature Geosci.* **2,** 419–422 (2009).
30. Labrosse, S. Thermal and magnetic evolution of the earth's core. *Phys. Earth Planet. Inter.* **140,** 127–143 (2003).

Supplementary Information is linked to the online version of the paper at www.nature.com/nature.

Acknowledgements This work has benefited from discussions during the CNRS-INSU SEDIT meetings. We thank M. Bergman for discussions regarding inner-core crystallization. The LGIT and the ANR (Agence Nationale de la Recherche) (ANR-08-BLAN-0234-01) have provided financial support for the experiments.

Author Contributions M.M., R.D. and T.A. ran and analysed the experiments. T.A. designed the experimental study and built the dynamical model. R.D. and T.A. worked out the thermal conditions on the ICB and assessed the geophysical relevance of the dynamical model. R.D. computed the different scenarios of thermal history. R.D., T.A. and M.M. applied the experimental results to the geophysical context. T.A. and R.D. wrote the paper.

Author Information Reprints and permissions information is available at www.nature.com/reprints. The authors declare no competing financial interests. Readers are welcome to comment on the online version of this article at www.nature.com/nature. Correspondence and requests for materials should be addressed to T.A. (thierry.alboussiere@ens-lyon.fr).

METHODS

We present here in some detail an analytical model of inner-core translation. The model results from the combination of three physical phenomena: the thermal state of the inner core, gravitational equilibrium and phase change restrictions due to finite heat exchange with the outer core.

Thermal evolution of the inner core. In the inner core, owing to secular cooling, any parcel of matter experiences a decrease in temperature with respect to its initial curve of constant entropy. However, as the inner core grows, newly solidified material is set to a lower and lower entropy value. Hence the inner core is thermally stable if formerly solidified matter is colder than the current adiabatic profile attached to the liquidus temperature at the ICB, as a result of diffusion. If not, it is unstable to thermal convection.

It is convenient to introduce a potential temperature $\Theta(\mathbf{r}, t) = T - T_{\rm ad}(r, t)$, where the adiabat $T_{\rm ad}(r, t)$ is anchored at the ICB (that is, $\Theta = 0$ at the ICB). At inner-core conditions, the equation of conservation of entropy can be simplified (see Supplementary Information) and written as

$$\frac{\partial \Theta}{\partial t} + (\mathbf{v}\cdot\nabla)\Theta = \kappa\nabla^2\Theta + S(t) \tag{7}$$

where κ is the thermal diffusivity of solid iron. This form of the entropy equation captures first-order effects of compressibility by retaining the contribution of adiabatic heating or cooling during vertical advection[31]. The source term is

$$S(t) = \kappa\nabla^2 T_{\rm ad} - \dot{T}_{\rm ad} \tag{8}$$

where $\dot{T}_{\rm ad} = \partial T_{\rm ad}/\partial t$ is the difference between thermal diffusion along the adiabat and secular cooling and is independent of space. The sign of S determines whether or not the inner core is superadiabatic and likely to convect. It is uncertain because S is the difference between two poorly constrained quantities of comparable magnitude. A young inner core (large secular cooling) and small thermal diffusivity favour a superadiabatic temperature regime (positive S) and instability. The low estimate of thermal conductivity given recently by Stacey and Davis[20] together with the young inner core age favoured by recent core thermal models[30, 32,33] make it plausible: with a conductivity $k = 36\,{\rm W\,m^{-1}\,K^{-1}}$ as suggested by ref. 20, the inner core would be superadiabatic if its age is of the order of a billion years or less. $S(t)$ can be calculated for any given thermal history of the core (see Supplementary Information); it is a decreasing function of time, with typical values of 10–100 K per billion years. In what follows, we assume that S is indeed positive, and will use a nominal value of $S = 10^{-15}\,{\rm K\,s^{-1}} \approx 30\,{\rm K}$ per billion years.

If it is superadiabatic, the inner core is mechanically unstable. Classical thermal convection will develop if the inner-core viscosity is not too large[34–36], but the fact that the ICB is not fixed allows for a new instability consisting of a translation (see Supplementary Information for a linear stability analysis). Under the assumption that the viscosity of the inner core is large enough, this mode becomes dominant and the motion is effectively restricted to be a translation, with velocity V. Assuming that the Péclet number (${\rm Pe} = Vc/\kappa$, where c is the radius of the inner core) is very large, the terms $\partial\Theta/\partial t$ and $\kappa\nabla^2\Theta$ can be neglected in equation (7), which now takes the simple form

$$\frac{\partial \Theta}{\partial x} = \frac{S}{V} \tag{9}$$

for a uniform velocity V in the direction of the x axis (see Fig. 3). With a boundary condition of $\Theta = 0$ on the crystallization side, the solution is

$$\Theta = \left(r\cos\theta + \sqrt{c^2 - r^2\sin^2\theta}\right)\frac{S}{V} \tag{10}$$

where r is the distance from the centre O of the inner core and θ is the angle between the x axis and the direction of the point where Θ is evaluated (see Fig. 3). The component Θ goes back to zero on the melting side within a thin boundary layer (not visible on the schematic Fig. 3) of thickness $\kappa/V \ll c$, which can be resolved when thermal diffusion is considered. The maximal temperature deviation from spherical symmetry is thus $\Delta T = 2cS/V$.

Mechanical equilibrium. The thermal asymmetry induced by a translation of the inner core is accompanied by a density asymmetry and it is anticipated that the inner core as a whole will be shifted in the direction of the thermal gradient in an attempt to move the centre of mass of the inner core towards the centre of the Earth: the light part is emerging while the dense part is sinking. We show here that a new equilibrium state with the inner core translated by a distance δ in the x direction results from a balance between the gravitational forces applied on the inner core and the pressure forces on the ICB. A correct estimate of the position of the inner core requires the evaluation of the change in self-gravitational potential resulting from the change in mass distribution.

For the sake of simplicity and tractability, density in the outer core is supposed to be uniform. In the inner core, density variations in the direction of the uniform velocity are kept in the analysis, but perpendicular variations are ignored. They would lead to degree 2 spherical harmonic contributions with little contribution to the displacement δ. Adiabatic spherical symmetric density variations are ignored because they contribute to δ only by slightly changing the average density of the inner core. Density in the inner core is thus expressed as

$$\rho = \rho_{\rm l} + (\rho_{\rm s} - \rho_{\rm l}) - \alpha\frac{S}{V}\rho_{\rm s} r\cos\theta \tag{11}$$

where α is the volume thermal expansion coefficient of the inner core, and $\rho_{\rm l}$ and $\rho_{\rm s}$ are the density of the liquid outer core and solid inner core. In equation (11), the first term on the right-hand side (that is, $\rho_{\rm l}$) is the contribution of the liquid core, centred on C, and the other two terms on the right-hand side are the contributions of the inner core, centred on O, separated from C by a distance δ. Let us introduce the gravitational potential U, such that gravity is $g = -\nabla U$, obeying the Poisson equation $\nabla^2 U = 4\pi G\rho$, with G the universal gravitational constant. From equation (11), the corresponding gravitational potential is found to be

$$\frac{U}{4\pi G} = \rho_{\rm l}\frac{R^2}{6} + (\rho_{\rm s} - \rho_{\rm l})\frac{r^2}{6} - \alpha\frac{S}{V}\rho_{\rm s}\left(\frac{r^3}{10} - \frac{c^2 r}{6}\right)\cos\theta \tag{12}$$

where r denotes the distance between the point at which U is calculated and the centre of the inner core O and R the distance between the same point and the centre of the Earth C (see Fig. 3). In the derivation of equation (12), the potential had to be determined inside and outside the inner core, whereas potential and gravity are continuous across the ICB. The formula (12) is the gravitational potential within the inner core. Noting that $R^2 = r^2 + 2\delta r\cos\theta + \delta^2$, equation (12) becomes

$$\frac{U}{4\pi G} = \rho_{\rm s}\frac{r^2}{6} + \rho_{\rm l}\frac{\delta^2}{6} - \alpha\frac{S}{V}\rho_{\rm s}\left(\frac{r^3}{10} - \frac{c^2 r}{6}\right)\cos\theta + \delta\,\rho_{\rm l}\frac{r}{3}\cos\theta \tag{13}$$

The total gravitational forces exerted on the inner core can be readily evaluated as

$$\mathbf{F}_G = -\int_{\text{inner core}} \rho\nabla U\,{\rm d}V = -4\pi G\,\delta\,\rho_{\rm l}\rho_{\rm s}\int_{\text{inner core}} \nabla\left(\frac{r}{3}\cos\theta\right){\rm d}V \tag{14}$$

Only the contribution from the last term in equation (13) remains, because the other terms cancel out or have no contribution. Indeed, the distribution of masses within the inner core exerts no net gravity force on the inner core itself and only the outer core has a non-zero contribution when the inner core is not centred. We finally obtain

$$\mathbf{F}_G = -\frac{16\,\pi^2}{9}\,G\,\delta\,\rho_{\rm l}\rho_{\rm s}c^3\,\mathbf{e}_x \tag{15}$$

Within the liquid outer core, we assume hydrostatic equilibrium $-\nabla P - \rho_{\rm l}\nabla U = 0$, which provides a simple relationship between pressure P and the potential U evaluated in equation (13)

$$P = -\rho_{\rm l}\,U \tag{16}$$

up to an additive constant. It is then possible to evaluate the net pressure force exerted by the outer core on the ICB

$$\mathbf{F}_P = -\oint_{\rm ICB} P\mathbf{e}_r{\rm d}S = \frac{16\,\pi^2}{9}\,G\,\rho_{\rm l}c^3\left[\alpha\frac{S}{V}\rho_{\rm s}\frac{c^2}{5} + \rho_{\rm l}\delta\right]\mathbf{e}_x \tag{17}$$

The net force exerted on the inner core is then

$$\mathbf{F} = \mathbf{F}_P + \mathbf{F}_G = \frac{16\,\pi^2}{9}G\rho_{\rm l}c^3\left[\alpha\frac{S}{V}\rho_{\rm s}\frac{c^2}{5} - (\rho_{\rm s} - \rho_{\rm l})\delta\right]\mathbf{e}_x \tag{18}$$

Static equilibrium of the inner core ($\mathbf{F} = \mathbf{0}$) is reached when the inner core is translated by a distance equal to

$$\delta = \frac{\alpha\frac{S}{V}\rho_{\rm s}c^2}{5(\rho_{\rm s} - \rho_{\rm l})} \tag{19}$$

Kinetics of phase change at the ICB. The displacement of the inner core implies that pressure is no longer uniform on the ICB. This corresponds to a temperature difference δT between the adiabat and the liquidus temperature along the interface:

$$\delta T = -\delta P(m_P - m_{\rm ad}) \tag{20}$$

where δP denotes the pressure variation on the ICB and m_P and $m_{\rm ad}$ are the Clapeyron slope and adiabatic gradient (in the liquid phase) respectively. Pressure variations on the ICB can readily be determined from the previous calculations on gravitational equilibrium. Pressure in the liquid is related to the gravitational potential (through equation (16)). The gravitational potential (13) is evaluated on the ICB $r = c$, with equation (19) taken into account

$$\frac{U}{4\pi G} = \frac{\rho_s}{6}\left[c^2 + \delta^2 + 2\,\delta c\cos\theta\right] \quad (21)$$

Hence, the pressure variation on the ICB follows from equations (16) and (21)

$$\delta P = -\rho_l g_c \delta\cos\theta \quad (22)$$

where $g_c = G\frac{4\pi}{3}\rho_s c$ is the gravitational acceleration in $r = c$. From equation (20), the temperature departure from the adiabat is

$$\delta T = \rho_l g_c\ \delta\ \cos\theta\ (m_P - m_{ad}) \quad (23)$$

The adiabat is thus higher than thermodynamic equilibrium on the eastern side and lower by the same amount on the western side. We do not assume that the actual temperature of the solid–liquid interface is dependent on the rate of melting or crystallization, dynamic undercooling being very small for metals. We consider instead that a thermal boundary layer develops in the outer core, which is the cause of heat exchange, that is, supply or extraction of latent heat (see Fig. 4). Heat conduction in the solid and in the liquid are smaller contributions and are fairly equal and opposite. Moreover, it is assumed that the rate of crystallization (and melting on the other side) is much bigger than the growth rate of the inner-core dc/dt, where $c(t)$ is the radius of the inner core. Fusion and crystallization are thus supposed to be of equal magnitude: this can be expressed in a single form $V\cos\theta$, where V is the assumed uniform velocity of the inner core. Heat transfer in the liquid outer core is related to the amplitude of velocity fluctuations u' in the outer core: we have little knowledge regarding u' near the ICB, so we take them to be of the same order of magnitude as the velocity at the core–mantle boundary estimated from the secular variation of the magnetic field, which is $10^{-4}\,\mathrm{m\,s^{-1}}$. The simplest estimate for the heat transfer coefficient is $c_p u'$. Hence, the heat budget at the ICB is

$$L\,V\cos\theta = u'\ c_p\ \delta T \quad (24)$$

where L is the latent heat. This equation relates the velocity V (rate of crystallization on one side, melting on the other side) to the thermal departure from the adiabat δT at the interface, which is itself related to the displacement δ of the inner core by equation (23).

Results of the model. All elements of the model have been analysed and now we put them together. Equations (23) and (24) provide a relationship between δ and V

$$L\ V = u' c_p \rho_l g_c (m_P - m_{ad})\delta \quad (25)$$

corresponding to the thermal aspect of the problem. Using the independent mechanical equation (19), the displacement δ can be eliminated and the solution for the translation velocity V can be obtained as

$$V^2 = \frac{4\pi G}{15}\frac{u'\ c_p \rho_s^2 \rho_l\ \alpha(m_P - m_{ad})S}{L(\rho_s - \rho_l)}\,c^3 \quad (26)$$

Representative values of the parameters involved are $G = 6.67 \times 10^{-11}\ \mathrm{m^3\,kg^{-1}\,s^{-2}}$, $u' = 10^{-4}\,\mathrm{m\,s^{-1}}$, $c_p = 850\,\mathrm{J\,kg^{-1}\,K^{-1}}$ (ref. 23), $\rho_s = 12{,}800\ \mathrm{kg\ m^{-3}}$ and $\rho_l = 12{,}200\ \mathrm{kg\ m^{-3}}$ (ref. 17), $\alpha = 1.1 \times 10^{-5}\,\mathrm{K^{-1}}$ (ref. 21), $m_P = 8.5 \times 10^{-9}\,\mathrm{K\,Pa^{-1}}$ (ref. 22), $m_{ad} = (\alpha T)/(\rho_l c_p) = 6 \times 10^{-9}\ \mathrm{K\ Pa^{-1}}$, $L = 900\,\mathrm{kJ\,kg^{-1}}$ (refs 24, 25), and $c = 1{,}221\,\mathrm{km}$ (ref. 17). With $S = 10^{-15}\,\mathrm{K\,s^{-1}}$, the translation velocity obtained for the present state of the inner core is found to be $V \simeq 7.7 \times 10^{-10}\ \mathrm{m\ s^{-1}}$, which is faster than the growth rate of the radius of the inner core by a factor of around 70. This is a justification for neglecting the growth of the inner core in the analysis. The associated displacement is derived from equations (25) or (19). Its value is $\delta \simeq 95$ m. The maximal temperature disequilibrium is $\delta T \simeq 0.01$ K, while the non-adiabatic temperature difference across the inner core is $\Delta T = 2cS/V \simeq 3.2$ K. Because δT is very small compared to ΔT, the boundary condition $\Theta = 0$ is justified to a good approximation from the point of view of the inner core. It is also possible to determine the maximal time of residence in the solid inner core, which is $2c/V \simeq 100$ million years.

31. Tritton, D. J. *Physical Fluid Dynamics* 1–536 (Oxford, Clarendon Press, 1988).
32. Gubbins, D., Alfè, D., Masters, G., Price, G. D. & Gillan, M. Gross thermodynamics of two-component core convection. *Geophys. J. Int.* **157,** 1407–1414 (2004).
33. Nimmo, F. in *Treatise on Geophysics* (ed. Schubert, G.) Vol. 2, 31–65, 2007).
34. Jeanloz, R. & Wenk, H.-R. Convection and anisotropy of the inner core. *Geophys. Res. Lett.* **15,** 72–75 (1988).
35. Weber, P. & Machetel, P. Convection within the inner-core and thermal implications. *Geophys. Res. Lett.* **19,** 2107–2110 (1992).
36. Wenk, H.-R., Baumgardner, J. R., Lebensohn, R. A. & Tomé, C. N. A convection model to explain anisotropy of the inner core. *J. Geophys. Res.* **105,** 5663–5678 (2000).